

1/f noise of a tiny tunnel magnetoresistance sensor originated from a wide distribution of bath correlation time

Hiroshi Imamura,* Hiroko Arai,† Rie Matsumoto, and Toshiki Yamaji

National Institute of Advanced Industrial Science and Technology (AIST),

Research Center for Emerging Computing Technologies (RCECT), Tsukuba, Ibaraki 305-8568, Japan

Tunnel magnetoresistance (TMR) sensor is a highly sensitive magnetic field sensor and is expected to be applied in various fields, such as magnetic recording, industrial sensing, and bio-medical sensing. To improve the detection capability of TMR sensors in low frequency regime it is necessary to suppress the 1/f noise. We theoretically study 1/f noise of a tiny TMR sensor using the macrospin model. Starting from the generalized Langevin equation, 1/f noise power spectrum and the Hooge parameter are derived. The calculated Hooge parameter of a tiny TMR sensor is much smaller than that of a conventional TMR sensor with large junction area. The results provide a new perspective on magnetic 1/f noise and will be useful for improvement of TMR sensors.

I. INTRODUCTION

Tunnel magnetoresistance (TMR) sensor [1–7] is a highly sensitive magnetic field sensor where the magnetic field signal is converted to the change in resistance of a magnetic tunnel junction (MTJ) [8–12]. The most popular application of the TMR sensor is a reading head of hard disk drives. Because of its high sensitivity, small size, and low power consumption, the TMR sensors are expanding their applications into a variety of fields such as industrial sensing and bio-medical sensing. In the bio-medical applications such as magnetocardiography and magnetoencephalography, TMR sensors detect the weak magnetic fields generated in the human heart and brain by electrophysiological activity of cardiac muscle and nerve cells [4–6]. The frequency range of the bio-magnetic signal is less than a few hundred Hz where the 1/f noise is the dominant noise. Reduction of 1/f noise is a key issue for bio-medical applications [3, 13].

1/f noise is a ubiquitous low-frequency noise whose noise power is inversely proportional to the frequency, f [14–17]. A large number of theories have been developed to explain the mechanism of 1/f noise as reviewed in Ref. [17]. An obvious way to obtain a 1/f power spectrum is to superimpose a large number of Lorentzian power spectra produced by exponential relaxation processes [14, 17–20]. The magnitude of the 1/f noise in different devices and materials is characterized by the Hooge parameter [15].

The magnetic 1/f noise derived from thermal fluctuation of magnetization in a TMR sensor has been studied by several groups [2, 7, 21–28]. In most previous studies the TMR sensors exhibit clear hysteresis in the magnetic field dependence of resistance, and the 1/f noise is observed within the hysteresis loop. The observed 1/f noise has been attributed to thermally excited hopping of magnetic domain walls between pinning sites. It is natural to ask the question if the magnetic 1/f noise appears in a

tiny TMR sensor where the domain wall cannot be created. If 1/f noise appears in a tiny TMR sensor, what is its power? To answer this question it is necessary to develop a theoretical model of magnetic 1/f noise based on the macrospin model.

In this paper, we propose a theoretical model for the magnetic 1/f noise of a tiny TMR sensor based on the macrospin model. Starting from the generalized Langevin equation, we derive an analytical expression of the voltage power spectrum in the low frequency regime. Assuming a wide distribution of bath correlation times, the derived voltage power spectrum is inversely proportional to the frequency, i.e. 1/f noise. We also show that the Hooge parameter of a tiny TMR sensor is much smaller than that of a conventional TMR sensors with large junction area.

II. THEORETICAL MODEL

The system we consider is the MTJ nano-pillar shown in Fig. 1 (a), which is the core element of a tiny TMR sensor. The nonmagnetic insulating layer is sandwiched by the ferromagnetic layers. The top ferromagnetic layer is the free layer (FL) of which magnetization is softly pinned by the orange peel coupling field, \mathbf{H}_p , directing in the z direction and by the uniaxial anisotropy field, H_k , along the z axis. The direction of the magnetization in the FL is denoted by \mathbf{m} . To tune the sensitivity, the bias field, \mathbf{H}_b , is applied in the y direction. The bottom ferromagnetic layer is the reference layer of which magnetization unit vector, \mathbf{p} , is fixed to the negative z direction [7]. The size of the TMR sensor is assumed to be so small that a domain wall cannot be created in the FL, i.e. about or less than 10 nm.

Assuming that the FL is a thin circular disk, the magnetic free energy density of the FL is given by

$$E = -\mu_0 M_s \mathbf{m} \cdot (\mathbf{H}_p + \mathbf{H}_b) + \frac{1}{2} \mu_0 M_s^2 m_x^2 - \frac{1}{2} \mu_0 M_s H_k m_z^2, \quad (1)$$

* h-imamura@aist.go.jp

† arai-h@aist.go.jp

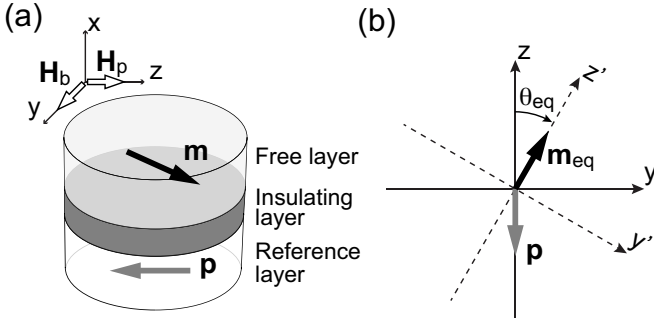


FIG. 1. (a) Schematic illustration of a magnetic tunnel junction. The insulating layer is sandwiched by the free layer (FL) and the reference layer (RL). The direction of the magnetization in the FL is denoted by the magnetization unit vector, \mathbf{m} . The direction of the magnetization in the RL is denoted by the magnetization unit vector, \mathbf{p} , and is fixed in the negative z direction. The magnetization in the FL is pinned by the orange peel coupling field, \mathbf{H}_p , directing in the z direction and by the uniaxial anisotropy field along the z axis.

The bias field, \mathbf{H}_b , is applied in the y direction. (b)

Definition of the rotated coordinate system. The z' axis is aligned to the equilibrium direction of the magnetization in the FL, \mathbf{m}_{eq} , by rotating around the x axis with the angle θ_{eq} .

where μ_0 is the permeability of vacuum, and M_s is the saturation magnetization. The equilibrium direction, $\mathbf{m}_{\text{eq}} = (0, \sin \theta_{\text{eq}}, \cos \theta_{\text{eq}})$, is obtained by minimizing E .

The voltage noise of the TMR sensor is induced by the resistance variation due to fluctuation of \mathbf{m} around the equilibrium direction. To calculate the fluctuation of \mathbf{m} we introduce the rotated coordinate system shown in Fig. 1(b), where the y' and z' axes are generated by rotating the y and z axes around the x axis by the angle θ_{eq} . The basis vectors of the $x-y'-z'$ coordinate system are defined as

$$\begin{pmatrix} \mathbf{e}_x \\ \mathbf{e}_{y'} \\ \mathbf{e}_{z'} \end{pmatrix} = \begin{pmatrix} 1 & 0 & 0 \\ 0 & \cos \theta_{\text{eq}} & -\sin \theta_{\text{eq}} \\ 0 & \sin \theta_{\text{eq}} & \cos \theta_{\text{eq}} \end{pmatrix} \begin{pmatrix} \mathbf{e}_x \\ \mathbf{e}_y \\ \mathbf{e}_z \end{pmatrix}. \quad (2)$$

In the rotated coordinate system, the magnetization unit vector in the FL is represented as

$$\mathbf{m} = m_x \mathbf{e}_x + m_{y'} \mathbf{e}_{y'} + m_{z'} \mathbf{e}_{z'}. \quad (3)$$

Since we are interested in the small fluctuation of \mathbf{m} around \mathbf{m}_{eq} , we assume $|m_x| \ll 1$, $|m_{y'}| \ll 1$, and $|m_{z'}| \simeq 1$.

The resistance of the TMR sensor is given by [8, 9, 29]

$$R = R_0 + \frac{\bar{R}}{1 + P^2 \mathbf{m} \cdot \mathbf{p}}, \quad (4)$$

where R_0 is the resistance not caused by tunneling, \bar{R} is the resistance due to tunneling at $\mathbf{m} \cdot \mathbf{p} = 0$, P is the spin polarization of tunneling electrons. Substituting Eq. (3)

into Eq. (4), the resistance is obtained as

$$R = R_0 + \frac{\bar{R}}{1 - P^2 (\cos \theta_{\text{eq}} m_{z'} - \sin \theta_{\text{eq}} m_{y'})}. \quad (5)$$

Up to the first order of $m_{y'}$, the resistance can be approximated as

$$R = R_0 + \frac{\bar{R}}{1 - P^2 \cos \theta_{\text{eq}}} - \frac{\bar{R} P^2 \sin \theta_{\text{eq}}}{(1 - P^2 \cos \theta_{\text{eq}})^2} m_{y'}. \quad (6)$$

III. RESULTS

In this section, we show the results of our theoretical analysis on magnetic $1/f$ noise of a tiny TMR sensor. We first show the relation between the voltage power spectrum and the power spectrum of $m_{y'}$ in Sec. III A. To calculate the power spectrum of $m_{y'}$, we solve the linearized equations of motion of \mathbf{m} by using the Fourier transformation in Sec. III B. Then we derive the Lorentzian power spectrum of $m_{y'}$ in Sec. III C. Assuming that bath correlation time, τ_c , has a wide distribution, we derive the $1/f$ power spectrum of voltage by superimposing the Lorentzian power spectra with different τ_c in Sec. III D. In Sec. III E, we show that the Hooge parameter of a tiny TMR sensor is much smaller than the conventional TMR sensor with the same sensitivity by comparing with the experimental results of Ref. [7].

A. Power spectrum of voltage

In most experiments, the voltage noise of a TMR sensor is measured under a constant direct current, I . Assuming that the measured voltage, V , is proportional to the resistance, R , the power spectrum of voltage, $S_{VV}(f)$, is proportional to the power spectrum of resistance, $S_{RR}(f)$, as

$$S_{VV}(f) = I^2 S_{RR}(f). \quad (7)$$

Introducing the angular frequency, $\omega = 2\pi f$, the power spectrum of resistance is defined as

$$S_{RR}(\omega) = 4 \int_0^\infty \langle R(t)R(0) \rangle \cos(\omega t) dt, \quad (8)$$

where $\langle \rangle$ represents the statistical average. Substituting Eq. (6) into Eq. (8), $S_{RR}(\omega)$ is expressed as

$$S_{RR}(\omega) = \left[\frac{\bar{R} P^2 \sin \theta_{\text{eq}}}{(1 - P^2 \cos \theta_{\text{eq}})^2} \right]^2 S_{m_{y'}, m_{y'}}(\omega), \quad (9)$$

where $S_{m_{y'}, m_{y'}}(\omega)$ is the power spectrum of $m_{y'}$ defined as

$$S_{m_{y'}, m_{y'}}(\omega) = 4 \int_0^\infty \langle m_{y'}(t)m_{y'}(0) \rangle \cos(\omega t) dt. \quad (10)$$

We define the Fourier transform of a function $f(t)$ as $f(\omega) = \int_{-\infty}^{\infty} f(t) \exp(-i\omega t) dt$. Substituting the inverse Fourier transform of $m_{y'}$ into Eq. (10) and performing some algebra, we obtain

$$S_{m_{y'} m_{y'}}(\omega) = \frac{1}{2\pi} \int_{-\infty}^{\infty} \langle m_{y'}(\omega) m_{y'}(\omega') \rangle d\omega' + \frac{1}{2\pi} \int_{-\infty}^{\infty} \langle m_{y'}(-\omega) m_{y'}(\omega') \rangle d\omega'. \quad (11)$$

The Fourier transform of $m_{y'}$ can be obtained by solving the equations of motion in the Fourier space.

B. Equations of motion and the Fourier transforms of m_x and $m_{y'}$

The equations of motion of \mathbf{m} is given by the following generalized Langevin equation [30–32],

$$\dot{\mathbf{m}}(t) = -\gamma \mathbf{m}(t) \times (\mathbf{H}_{\text{eff}} + \mathbf{r}) + \alpha \mathbf{m} \times \int_{-\infty}^t \nu(t-t') \dot{\mathbf{m}}(t') dt', \quad (12)$$

where $\dot{\mathbf{m}}(t)$ is the time derivative of $\mathbf{m}(t)$, γ is the gyromagnetic ratio, and α is the Gilbert damping constant. The effective magnetic field acting on \mathbf{m} is given by

$$\mathbf{H}_{\text{eff}} = -M_s m_x \mathbf{e}_x + H_b \mathbf{e}_y + (H_p + H_k m_z) \mathbf{e}_z. \quad (13)$$

The memory function is defined as

$$\nu(t-t') = \frac{1}{\tau_c} \exp\left(-\frac{|t-t'|}{\tau_c}\right), \quad (14)$$

where τ_c is the bath correlation time. The thermal agitation field, \mathbf{r} , is a random field satisfying $\langle r_j \rangle = 0$ and

$$\langle r_j r_k \rangle = \frac{\mu}{2} \delta_{j,k} \nu(t-t'), \quad (15)$$

where subscripts j and k denotes x, y, z, y' , or z' . The constant μ is defined as

$$\mu = \frac{2\alpha k_B T}{\gamma \mu_0 M_s \Omega}, \quad (16)$$

where k_B is the Boltzmann constant, T is temperature, and Ω is the volume of the FL. From Eqs. (15) and (16) we see that the magnitude of the thermal agitation field is of the order of $\sqrt{\alpha}$ because μ is of the order of α . The stochastic LLG equation with the Markovian damping derived by Brown [33] is reproduced in the limit of $\tau_c \rightarrow 0$ because $\lim_{\tau_c \rightarrow 0} \nu(t-t') = 2\delta(t-t')$, where $\delta(t-t')$ is Dirac's delta function. It should be noted that $1/f$ noise cannot be derived from the LLG equation with the Markovian damping because many physical processes with different time scale is required to generate $1/f$ noise.

Since the FL of a typical TMR sensor is made of a ferromagnetic material with $\alpha \ll 1$, we focus on terms up

to the first order of α in the equations of motion. We also assume that $m_x, m_{y'}, r_x, r_{y'}$, and $r_{z'}$ are small enough to linearize the equations of motion in terms of these small variables. Equation (12) can be approximated as

$$\dot{m}_x(t) = -\omega_0 m_{y'}(t) + \gamma r_{y'}(t) - \alpha \int_{-\infty}^t \nu(t-t') \dot{m}_{y'}(t') dt' \quad (17)$$

$$\dot{m}_{y'}(t) = \omega_1 m_x(t) - \gamma r_x(t) + \alpha \int_{-\infty}^t \nu(t-t') \dot{m}_x(t') dt' \quad (18)$$

$$\dot{m}_{z'}(t) = 0, \quad (19)$$

where

$$\omega_0 = \gamma (H_b \sin \theta_{\text{eq}} + H_p \cos \theta_{\text{eq}} + H_k \cos 2\theta_{\text{eq}}), \quad (20)$$

$$\omega_1 = \gamma (M_s + H_b \sin \theta_{\text{eq}} + H_p \cos \theta_{\text{eq}} + H_k \cos^2 \theta_{\text{eq}}). \quad (21)$$

Following Ref. [32], we approximate the non-Markovian damping term in Eqs. (17) and (18) up to the first order of α . Successive application of the integration by parts gives the following linearized equations of motion up to the order of α ,

$$\dot{m}_x(t) = -\hat{\gamma}_1 \omega_0 m_{y'}(t) + \gamma r_{y'}(t) - \tilde{\alpha} \omega_1 m_x(t) \quad (22)$$

$$\dot{m}_{y'}(t) = \hat{\gamma}_0 \omega_1 m_x(t) - \gamma r_x(t) - \tilde{\alpha} \omega_0 m_{y'}(t), \quad (23)$$

where

$$\hat{\gamma}_0 = \left(1 + \frac{\alpha \xi_0}{1 + \xi_0 \xi_1}\right) \quad (24)$$

$$\hat{\gamma}_1 = \left(1 + \frac{\alpha \xi_1}{1 + \xi_0 \xi_1}\right) \quad (25)$$

$$\tilde{\alpha} = \frac{\alpha}{1 + \xi_0 \xi_1} \quad (26)$$

$$\xi_0 = \tau_c \omega_0$$

$$\xi_1 = \tau_c \omega_1. \quad (27)$$

Details of the derivation of the above equations will be provided in Appendix A. In the Fourier space, the equations of motion are expressed as

$$i\omega m_x(\omega) = -\hat{\gamma}_1 \omega_0 m_{y'}(\omega) + \gamma r_{y'}(\omega) - \tilde{\alpha} \omega_1 m_x(\omega), \quad (28)$$

$$i\omega m_{y'}(\omega) = \hat{\gamma}_0 \omega_1 m_x(\omega) - \gamma r_x(\omega) - \tilde{\alpha} \omega_0 m_{y'}(\omega). \quad (29)$$

The solutions are obtained as

$$m_x(\omega) = \frac{\hat{\gamma}_1 \omega_0 \gamma r_{y'}(\omega) + (\tilde{\alpha} \omega_0 + i\omega) \gamma r_{y'}(\omega)}{A(\omega)} \quad (30)$$

$$m_{y'}(\omega) = \frac{\hat{\gamma}_0 \omega_1 \gamma r_{y'}(\omega) - (\tilde{\alpha} \omega_1 + i\omega) \gamma r_x(\omega)}{A(\omega)}, \quad (31)$$

where

$$A(\omega) = (\hat{\gamma}_0 \hat{\gamma}_1 + \tilde{\alpha}^2) \omega_0 \omega_1 - \omega^2 + i\tilde{\alpha}(\omega_0 + \omega_1)\omega. \quad (32)$$

C. Power spectrum of $m_{y'}$

From Eq. (31), the correlation of $m_{y'}(\omega)$ and $m_{y'}(\omega')$ is expressed as

$$\begin{aligned} \langle m_{y'}(\omega)m_{y'}(\omega') \rangle &= \frac{(\hat{\gamma}_0\omega_1)^2}{A(\omega)A(\omega')} \gamma^2 \langle r_{y'}(\omega)r_{y'}(\omega') \rangle \\ &+ \frac{(\tilde{\alpha}\omega_1 + i\omega)(\tilde{\alpha}\omega_1 + i\omega')}{A(\omega)A(\omega')} \gamma^2 \langle r_x(\omega)r_x(\omega') \rangle, \end{aligned} \quad (33)$$

where we use the fact that r_x and $r_{y'}$ do not correlate with each other. The correlation $\langle m_{y'}(-\omega)m_{y'}(\omega') \rangle$ is obtained by replacing ω with $-\omega$ in Eq. (33)

Following Ref. [34], the correlation of thermal agitation fields in the Fourier space is obtained as

$$\langle r_j(\omega)r_k(\omega') \rangle = 2\pi\mu\delta_{j,k} \frac{1}{1+i\tau_c\omega} \delta(\omega+\omega'). \quad (34)$$

The correlation $\langle r_j(-\omega)r_k(\omega') \rangle$ is obtained by replacing ω with $-\omega$ in Eq. (34).

Substituting Eqs. (33) and (34) into Eq. (11), the power spectrum of $m_{y'}$ is expressed as

$$S_{m_{y'}m_{y'}}(\omega) = \frac{(\hat{\gamma}_0^2 + \tilde{\alpha}^2)\omega_1^2 + \omega^2}{B(\omega)} \frac{2\gamma^2\mu}{1 + (\tau_c\omega)^2}, \quad (35)$$

where

$$\begin{aligned} B(\omega) &= [(\hat{\gamma}_0\hat{\gamma}_1 + \tilde{\alpha}^2)\omega_0\omega_1 - \omega^2]^2 \\ &+ [\tilde{\alpha}(\omega_0 + \omega_1)\omega]^2. \end{aligned} \quad (36)$$

In the low frequency regime satisfying $\omega \ll \omega_0$ and $\omega \ll \omega_1$, Eq. (35) can be approximated by the Lorentzian function as

$$S_{m_{y'}m_{y'}}(\omega) = \frac{2\gamma^2\mu}{(\hat{\gamma}_1\omega_0)^2} \frac{1}{1 + (\tau_c\omega)^2}. \quad (37)$$

Since ω_0 and ω_1 are of the order of 0.1 GHz \sim 10 GHz for conventional TMR sensors [7], the low frequency condition is clearly satisfied for the frequency range of the bio-magnetic signal, i.e. less than a few hundred Hz.

D. Superimposition of Lorentzian power spectra

Bath correlation time, τ_c , is the decay time of the correlation of thermal agitation field as shown in Eq. (15). Thermal agitation field is produced by many kinds of sources or baths such as dipolar coupling with magnons in the reference layer and spin orbit coupling with phonons. Since τ_c depends on the relaxation mechanism of the bath, different relaxation modes in different baths have their own τ_c . Instead of discussing τ_c for some specific types of baths, we just assume a distribution of τ_c and analyze the effect of the distribution of τ_c on the low frequency power spectrum of voltage. Assuming a wide

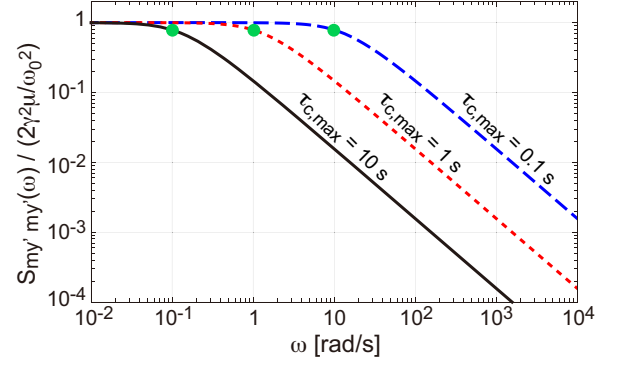


FIG. 2. Power spectrum of $m_{y'}$, $S_{m_{y'}m_{y'}}(\omega)$ given by Eq. (40) normalized by $2\gamma^2\mu/\omega_0^2$. The black solid, red dotted, and blue dashed curves represent the results for $\tau_{c,max}=10, 1,$ and 0.1 s, respectively. The green circles indicate the values at $\omega = 1/\tau_{c,max}$.

distribution of τ_c , we derive an analytical expression of the power spectrum of the magnetic $1/f$ noise.

We assume that τ_c is uniformly distributed in the range of $\tau_{c,min} \leq \tau_c \leq \tau_{c,max}$ and has the probability distribution defined as $\rho(\tau_c) = 1/(\tau_{c,max} - \tau_{c,min})$. The superimposition of $S_{m_{y'}m_{y'}}(\omega)$ for all τ_c is given by

$$S_{m_{y'}m_{y'}}(\omega) = \frac{2\gamma^2\mu}{\omega_0^2} \int_0^\infty \frac{1}{\hat{\gamma}_1^2} \frac{\rho(\tau_c)}{1 + (\tau_c\omega)^2} d\tau_c. \quad (38)$$

As a function of τ_c , $\hat{\gamma}_1$ is almost unity except around the peak at $\tau_c = 1/\sqrt{\omega_0\omega_1}$, which is of the order of ns. Since the peak value of $\hat{\gamma}_1$ is as small as $1 + (\alpha/2)\sqrt{\omega_1/\omega_0}$, and ω is assumed to be much smaller than ω_0 and ω_1 , Eq. (38) can be approximated as

$$\begin{aligned} S_{m_{y'}m_{y'}}(\omega) &= \frac{2\gamma^2\mu}{\omega_0^2} \frac{1}{\tau_{c,diff}} \int_{\tau_{c,min}}^{\tau_{c,max}} \frac{1}{1 + (\tau_c\omega)^2} d\tau_c \\ &= \frac{2\gamma^2\mu}{\omega_0^2} \frac{1}{\tau_{c,diff}} \left[\frac{\arctan(\omega\tau_{c,max})}{\omega} \right. \\ &\quad \left. - \frac{\arctan(\omega\tau_{c,min})}{\omega} \right], \end{aligned} \quad (39)$$

where $\tau_{c,diff} = \tau_{c,max} - \tau_{c,min}$. Since $\arctan(x)/x$ is a monotonically decreasing function of x for $x > 0$ and $\lim_{x \rightarrow 0} \arctan(x)/x = 1$, $S_{m_{y'}m_{y'}}(\omega)$ is a monotonically decreasing function of ω and take a maximum value of $2\gamma^2\mu/\omega_0^2$ in the limit of $\omega \rightarrow 0$.

When $\omega\tau_{c,min} \ll 1$, the second term in the square bracket of Eq. (39) can be neglected and $S_{m_{y'}m_{y'}}(\omega)$ is approximated as

$$S_{m_{y'}m_{y'}}(\omega) = \frac{2\gamma^2\mu}{\omega_0^2} \frac{\arctan(\omega\tau_{c,max})}{\omega\tau_{c,max}}. \quad (40)$$

Figure 2 shows $S_{m_{y'}m_{y'}}(\omega)$ given by Eq. (40) normalized by $2\gamma^2\mu/\omega_0^2$ for $\tau_{c,max}=10$ s (black solid), 1 s (red dotted), and 0.1 s (blue dashed). The values at $\omega = 1/\tau_{c,max}$

are indicated by the green circles. All curves are almost flat for $\omega \ll 1/\tau_{c,\max}$ and inversely proportional to ω for $\omega \gg 1/\tau_{c,\max}$.

Assuming a wide distribution of τ_c satisfying $\omega\tau_{c,\min} \ll 1$ and $\omega\tau_{c,\max} \gg 1$, we have $\arctan(\omega\tau_{c,\min}) = 0$ and $\arctan(\omega\tau_{c,\max}) = \pi/2$. Then the power spectrum can be approximated as

$$S_{m_y, m_y'}(\omega) = \frac{2\gamma^2\mu}{\omega_0^2} \frac{1}{\tau_{c,\max}} \frac{\pi}{2\omega}, \quad (41)$$

which is inversely proportional to the angular frequency, $\omega (=2\pi f)$. From Eqs. (7), (9) and (41) the voltage power spectrum is given by

$$S_{VV}(f) = \left[\frac{I\bar{R}P^2 \sin \theta_{\text{eq}}}{(1 - P^2 \cos \theta_{\text{eq}})^2} \right]^2 \frac{\gamma^2\mu}{2\omega_0^2} \frac{1}{\tau_{c,\max}} \frac{1}{f}. \quad (42)$$

This is the main result of this paper. The obvious difference from other models of low frequency magnetic noise [21, 23, 35–38] is that Eq. (42) has the term $1/\tau_{c,\max}$ as information of the distribution of the bath correlation time. It should be noted that the $1/f$ noise of a tiny TMR sensor we derived is response to the thermal agitation fields that exhibit $1/f$ power spectrum as the superimposition of the Lorentzian power spectrum.

E. Comparison with a conventional TMR sensor with large junction area

We compare the derived $1/f$ noise of the macrospin model with the experimental results of a conventional TMR sensor with large junction area reported in Ref. [7]. The Hooke parameter, α_H , is a convenient measure to compare the $1/f$ noise between different MTJs, which is defined as

$$S_{VV}(f) = S_{VV}^{\text{wh}} + \alpha_H V_b^2 A^{-1} f^{-1}, \quad (43)$$

where S_{VV}^{wh} is the power spectral density of the white noise, V_b is the bias voltage, and A is the area of the MTJ. The typical value of the Hooke parameter of conventional TMR sensors is about $10^{-6} \sim 10^{-11} \mu\text{m}^2$ [7, 26–28]. From Eq. (6), the bias voltage is given by

$$V_b = I \left(R_0 + \frac{\bar{R}}{1 - P^2 \cos \theta_{\text{eq}}} \right). \quad (44)$$

From Eqs. (16), (42), (43), and (44), the Hooke parameter of a tiny TMR sensor is obtained as

$$\alpha_H = \left\{ \frac{\bar{R}P^2 \sin \theta_{\text{eq}}}{(1 - P^2 \cos \theta_{\text{eq}}) [\bar{R} + R_0(1 - P^2 \cos \theta_{\text{eq}})]} \right\}^2 \times \frac{\alpha \gamma k_B T}{\mu_0 M_s d} \frac{1}{\omega_0^2} \frac{1}{\tau_{c,\max}}, \quad (45)$$

where d is the thickness of the FL.

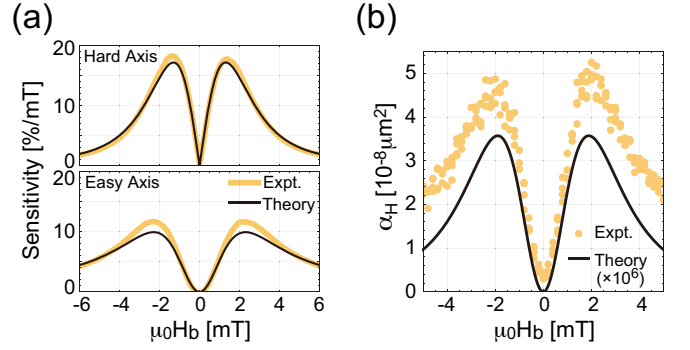


FIG. 3. (a) Sensitivity as a function of the bias field, $\mu_0 H_b$. The top panel shows the results for the signal field along the magnetization hard axis, i.e the y axis. The bottom panel shows the results for the signal field along the magnetization easy axis, i.e z axis. In both panels, the yellow and the black curves represent the experimental and theoretical results, respectively. (b) Hooke parameter, α_H , as a function of the bias field, $\mu_0 H_b$. The yellow circles and the black curve represent the experimental and theoretical results, respectively. Note that the theoretical results are multiplied by 10^6 . In all panels, the experimental results are the same as those shown in Fig. 3(b) in Ref. [7].

To compare Eq. (45) with the experimental results of a conventional TMR sensor, we determine the junction parameters by fitting the bias field dependence of the resistance shown in Figs. 2(a) of Ref. [7]. The parameters are determined as $M_s=0.93$ MA/m, $\mu_0 H_k=1.0$ mT, $\mu_0 H_p=2.15$ mT, $R_0=10.7 \Omega$, $\bar{R}=10.3 \Omega$, $P^2=0.74$. Figure 3(a) shows the bias field, $\mu_0 H_b$, dependence of the sensitivity defined as

$$\text{Sensitivity} = \frac{1}{R_{\max}} \frac{dR}{d\mu_0 H_b}, \quad (46)$$

where R_{\max} is the maximum value of the resistance. The experimental results indicated by the yellow curves are well reproduced by the theoretical results represented by the black curves.

Figure 3(b) shows the bias field dependence of the Hooke parameter, α_H . The experimental results are indicated by the yellow circles. The black solid curve represents the theoretical results multiplied by 10^6 . For calculation of the Hooke parameter, the following parameters are assumed: $\alpha = 0.05$, $d = 2$ nm, $\tau_{c,\max} = 1$ s, and $T = 300$ K. The field dependences of the Hooke parameter and the sensitivity look very similar because the Hooke parameter is proportional to the square of the sensitivity along the y' axis as indicated by Eqs. (6), (42), and (46).

The results show that the Hooke parameter of a tiny TMR sensor is much smaller than that of the conventional TMR sensor with the same sensitivity by a factor of 10^{-6} . If a number of tiny MTJs are connected in parallel to reproduce the same resistance as a conventional TMR sensor, the power spectrum of the magnetic $1/f$ noise can be reduced by a factor of 10^{-6} without reducing sensitivity.

IV. SUMMARY

In summary, we propose a theoretical model for magnetic $1/f$ noise of a tiny TMR sensor originated from distribution of bath correlation time. Starting from the generalized Langevin equation, we derive an analytical expression of the low frequency power spectrum of voltage. Assuming a wide distribution of the bath correlation times, the derived voltage power spectrum is inversely proportional to the frequency. We also show that the Hooge parameter of a tiny TMR sensor is much smaller than that of a conventional TMR sensor with large junction area. The power spectrum of the $1/f$ noise can be substantially reduced without reducing sensitivity by connecting tiny TMR sensors in parallel. The results provides a new perspective on magnetic $1/f$ noise and will be useful for reduction of $1/f$ noise of TMR sensors. The presented theoretical framework is applicable not only to the magnetic $1/f$ noise of a tiny TMR sensor, but also to the low frequency fluctuation of any tiny magnetic devices where the macrospin model is appropriate.

ACKNOWLEDGMENTS

The authors thank T. Nakatani for providing experimental data and for valuable discussions. This work was partly supported by JSPS KAKENHI Grant No. JP23K04575.

Appendix A: Derivation of Eqs. (22) and (23)

In this section, we provide the details of the derivation of Eqs. (22) and (23). Following Ref. [32], different approaches are used depending on the value of τ_c : in the short τ_c regime and in the long τ_c regime. Introducing $\xi_0 = \tau_c \omega_0$ and $\xi_1 = \tau_c \omega_1$, the short τ_c regime is defined as $\xi_0 \xi_1 < 1$, and the long τ_c regime is defined as $\xi_0 \xi_1 > 1$. For both τ_c regimes we can derive the same equations of motion as Eqs. (22) and (23).

a. Short τ_c regime: $\xi_0 \xi_1 < 1$

We approximate the non-Markovian damping term in Eq. (17) up to the first order of α . Successive application of the integration by parts using $\nu(t-t') = \tau_c [d\nu(t-t')/dt']$ the integral part of the non-Markovian damping term in Eq. (17) is expressed as

$$\int_{-\infty}^t \nu(t-t') \dot{m}_{y'}(t') dt' = \sum_{n=1}^{\infty} (-\tau_c)^{n-1} \frac{d^n}{dt^n} m_{y'}(t). \quad (\text{A1})$$

Since the integral part of the non-Markovian damping is multiplied by α we approximate the time derivative of

$m_{y'}(t)$ in the 0th order of α as

$$\frac{d^{2n}}{dt^{2n}} m_{y'}(t) = (-1)^n \omega_0^n \omega_1^n m_{y'}(t), \quad (\text{A2})$$

and

$$\frac{d^{2n+1}}{dt^{2n+1}} m_{y'}(t) = (-1)^n \omega_0^n \omega_1^{n+1} m_x(t). \quad (\text{A3})$$

Substituting Eqs. (A2) and (A3) into Eq. (A1), the integral part of the non-Markovian damping term in Eq. (17) is expressed as

$$\int_{-\infty}^t \nu(t-t') \dot{m}_{y'}(t') dt' = \left[\xi_1 \omega_0 m_{y'}(t) + \omega_1 m_x(t) \right] \sum_{n=1}^{\infty} (-\xi_0 \xi_1)^{n-1}. \quad (\text{A4})$$

The summation in Eq. (A4) converges under the condition of $\xi_0 \xi_1 < 1$ as

$$\sum_{n=1}^{\infty} (-\xi_0 \xi_1)^{n-1} = \frac{1}{1 + \xi_0 \xi_1}. \quad (\text{A5})$$

Then Eq. (A4) becomes

$$\int_{-\infty}^t \nu(t-t') \dot{m}_{y'}(t') dt' = \frac{\xi_1 \omega_0 m_{y'}(t) + \omega_1 m_x(t)}{1 + \xi_0 \xi_1}. \quad (\text{A6})$$

Substituting Eq. (A6) into Eq. (17) and performing some algebra, we obtain the following linearized equation of motion for $m_x(t)$ up to the first order of α :

$$\begin{aligned} \dot{m}_x(t) = & - \left(1 + \frac{\alpha \xi_1}{1 + \xi_0 \xi_1} \right) \omega_0 m_{y'}(t) \\ & + \gamma r_{y'}(t) - \frac{\alpha}{1 + \xi_0 \xi_1} \omega_1 m_x(t). \end{aligned} \quad (\text{A7})$$

Similarly the following linearized equation of motion for $m_{y'}(t)$ up to the first order of α is obtained as

$$\begin{aligned} \dot{m}_{y'}(t) = & \left(1 + \frac{\alpha \xi_0}{1 + \xi_0 \xi_1} \right) \omega_1 m_x(t) \\ & - \gamma r_x(t) - \frac{\alpha}{1 + \xi_0 \xi_1} \omega_0 m_{y'}(t). \end{aligned} \quad (\text{A8})$$

Using the symbols defined by Eqs. (24), (25), and (26), one can easily confirm that Eqs. (A7) and (A8) are the same as Eqs. (22) and (23), respectively.

b. Long τ_c regime: $\xi_0 \xi_1 > 1$

In the long bath τ_c regime satisfying $\xi_0 \xi_1 > 1$, we expand Eq. (17) in power series of $1/(\xi_0 \xi_1)$. Using the integration by parts with $d\nu(t-t')/dt' = \nu(t-t')/\tau_c$ the

integral part of the non-Markovian damping in Eq. (17) can be written as

$$\int_{-\infty}^t \nu(t-t') \dot{m}_{y'}(t') dt' = \frac{1}{\tau_c} \int_{-\infty}^t \dot{m}_{y'}(t') dt' - \frac{1}{\tau_c} \int_{-\infty}^t \nu(t-t') \left[\int_{-\infty}^{t'} \dot{m}_{y'}(t'') dt'' \right] dt'. \quad (\text{A9})$$

Successive application of the integration by parts gives

$$\int_{-\infty}^t \nu(t-t') \dot{m}_{y'}(t') dt' = - \sum_{n=1}^{\infty} \left(-\frac{1}{\tau_c} \right)^n J_n, \quad (\text{A10})$$

where J_n is the n th order multiple integral defined as

$$J_n = \int_{-\infty}^t \int_{-\infty}^{t_1} \cdots \int_{-\infty}^{t_{n-1}} \dot{m}_{y'}(t_n) dt_n \cdots dt_2 dt_1. \quad (\text{A11})$$

From Eq. (A2), on the other hand, $\dot{m}_{y'}(t)$ is expressed as

$$\dot{m}_{y'}(t) = \frac{1}{(-1)^n \omega_0^n \omega_1^n} \left(\frac{d^{2n+1}}{dt^{2n+1}} m_{y'}(t) \right). \quad (\text{A12})$$

Substituting Eq. (A12) into Eq. (A11) the multiple integrals are calculated as

$$J_{2n} = \frac{1}{(-1)^n \omega_0^n \omega_1^n} \dot{m}_{y'}(t), \quad (\text{A13})$$

and

$$J_{2n-1} = \frac{1}{(-1)^n \omega_0^n \omega_1^n} \ddot{m}_{y'}(t). \quad (\text{A14})$$

Substituting the time derivative of $m_{y'}(t)$ in the 0th order of α into Eqs. (A13) and (A14), we obtain

$$J_{2n} = \frac{\omega_1 m_x(t)}{(-1)^n \omega_0^n \omega_1^n}, \quad (\text{A15})$$

and

$$J_{2n-1} = \frac{m_{y'}(t)}{(-1)^{n-1} \omega_0^{n-1} \omega_1^{n-1}}. \quad (\text{A16})$$

Substituting Eqs. (A15) and (A16) into Eq. (A10) and performing some algebra, the integral part of the non-Markovian damping in Eq. (17) can be expressed as

$$\begin{aligned} & \int_{-\infty}^t \nu(t-t') \dot{m}_{y'}(t') dt' \\ &= - \sum_{n=1}^{\infty} \left[\left(-\frac{1}{\tau_c} \right)^{2n-1} J_{2n-1} + \left(-\frac{1}{\tau_c} \right)^{2n} J_{2n} \right] \\ &= - \left[\sum_{n=1}^{\infty} \left(-\frac{1}{\xi_0 \xi_1} \right)^n \right] [\xi_1 \omega_0 m_{y'}(t) + \omega_1 m_x(t)] \\ &= \frac{1}{1 + \xi_0 \xi_1} [\xi_1 \omega_0 m_{y'}(t) + \omega_1 m_x(t)]. \end{aligned} \quad (\text{A17})$$

In the last equality, we use the following relation:

$$\sum_{n=1}^{\infty} \left(-\frac{1}{\xi_0 \xi_1} \right)^n = -\frac{1}{1 + \xi_0 \xi_1}, \quad (\text{A18})$$

which holds under the condition that $\xi_0 \xi_1 > 1$. Equation (A17) is the same as Eq. (A6). Substituting Eq. (A17) into Eq. (17) and performing some algebra, we obtain the same linearized equation of motion of $m_x(t)$ as Eq. (22). Equation (23) can also be obtained by similar calculations.

-
- [1] P. P. Freitas, R. Ferreira, S. Cardoso, and F. Cardoso, Magnetoresistive sensors, *Journal of Physics: Condensed Matter* **19**, 165221 (2007).
- [2] W. Egelhoff, P. Pong, J. Unguris, R. McMichael, E. Nowak, A. Edelstein, J. Burnette, and G. Fischer, Critical challenges for picoTesla magnetic-tunnel-junction sensors, *Sensors and Actuators A: Physical* **155**, 217 (2009).
- [3] Z. Q. Lei, G. J. Li, W. F. Egelhoff, P. T. Lai, and P. W. T. Pong, Review of Noise Sources in Magnetic Tunnel Junction Sensors, *IEEE Transactions on Magnetics* **47**, 602 (2011).
- [4] K. Fujiwara, M. Oogane, A. Kanno, M. Imada, J. Jono, T. Terauchi, T. Okuno, Y. Aritomi, M. Morikawa, M. Tsuchida, N. Nakasato, and Y. Ando, Magnetocardiography and magnetoencephalography measurements at room temperature using tunnel magneto-resistance sensors, *Applied Physics Express* **11**, 023001 (2018).
- [5] M. Wang, Y. Wang, L. Peng, and C. Ye, Measurement of Triaxial Magnetocardiography Using High Sensitivity Tunnel Magnetoresistance Sensor, *IEEE Sensors Journal* **19**, 9610 (2019).
- [6] M. Oogane, K. Fujiwara, A. Kanno, T. Nakano, H. Wa-gatsuma, T. Arimoto, S. Mizukami, S. Kumagai, H. Matsuzaki, N. Nakasato, and Y. Ando, Sub-pT magnetic field detection by tunnel magneto-resistive sensors, *Applied Physics Express* **14**, 123002 (2021).
- [7] T. Nakatani, H. Suto, P. D. Kulkarni, H. Iwasaki, and Y. Sakuraba, Tunnel magnetoresistance sensors with symmetric resistance-field response and noise properties under AC magnetic field modulation, *Applied Physics Letters* **121**, 192406 (2022).

- [8] M. Julliere, Tunneling between ferromagnetic films, *Physics Letters A* **54**, 225 (1975).
- [9] S. Maekawa and U. Gafvert, Electron tunneling between ferromagnetic films, *IEEE Transactions on Magnetics* **18**, 707 (1982).
- [10] T. Miyazaki and N. Tezuka, Giant magnetic tunneling effect in Fe/Al₂O₃/Fe junction, *Journal of Magnetism and Magnetic Materials* **139**, L231 (1996).
- [11] S. S. P. Parkin, C. Kaiser, A. Panchula, P. M. Rice, B. Hughes, M. Samant, and S.-H. Yang, Giant tunnelling magnetoresistance at room temperature with MgO (100) tunnel barriers, *Nature Materials* **3**, 862 (2004).
- [12] S. Yuasa, T. Nagahama, A. Fukushima, Y. Suzuki, and K. Ando, Giant room-temperature magnetoresistance in single-crystal Fe/MgO/Fe magnetic tunnel junctions, *Nature Materials* **3**, 868 (2004).
- [13] M. Pannetier, C. Fermon, G. L. Goff, J. Simola, E. Kerr, and J. Coey, Noise in small magnetic systems—applications to very sensitive magnetoresistive sensors, *Journal of Magnetism and Magnetic Materials* **290-291**, 1158 (2005).
- [14] A. L. McWhorter, *1/f noise and germanium surface properties* (University of Pennsylvania Press, 1957) pp. 207–228.
- [15] F. N. Hooge, T. G. M. Kleinpenning, and L. K. J. Vandamme, Experimental studies on 1/f noise, *Reports on Progress in Physics* **44**, 479 (1981).
- [16] P. Dutta and P. M. Horn, Low-frequency fluctuations in solids: 1/f noise, *Reviews of Modern Physics* **53**, 497 (1981).
- [17] M. B. Weissman, 1/f noise and other slow, non exponential kinetics in condensed matter, *Reviews of Modern Physics* **60**, 537 (1988).
- [18] J. Bernamont, Fluctuations in the resistance of thin films, *Proceedings of the Physical Society* **49**, 138 (1937).
- [19] F. K. D. Pré, A Suggestion Regarding the Spectral Density of Flicker Noise, *Physical Review* **78**, 615 (1950).
- [20] A. V. D. Ziel, On the noise spectra of semi-conductor noise and of flicker effect, *Physica* **16**, 359 (1950).
- [21] S. Ingvarsson, G. Xiao, S. S. P. Parkin, W. J. Gallagher, G. Grinstein, and R. H. Koch, Low-Frequency Magnetic Noise in Micron-Scale Magnetic Tunnel Junctions, *Physical Review Letters* **85**, 3289 (2000).
- [22] C. Ren, X. Liu, B. D. Schrag, and G. Xiao, Low-frequency magnetic noise in magnetic tunnel junctions, *Physical Review B* **69**, 104405 (2004).
- [23] L. Jiang, E. R. Nowak, P. E. Scott, J. Johnson, J. M. Slaughter, J. J. Sun, and R. W. Dave, Low-frequency magnetic and resistance noise in magnetic tunnel junctions, *Physical Review B* **69**, 054407 (2004).
- [24] A. Gokce, E. R. Nowak, S. H. Yang, and S. S. P. Parkin, 1/f noise in magnetic tunnel junctions with MgO tunnel barriers, *Journal of Applied Physics* **99**, 08A906 (2006).
- [25] J. M. Almeida, R. Ferreira, P. P. Freitas, J. Langer, B. Ocker, and W. Maass, 1/f noise in linearized low resistance MgO magnetic tunnel junctions, *Journal of Applied Physics* **99**, 08B314 (2006).
- [26] Silva, Ana V., Leitao, Diana C., Valadeiro, João, Amaral, José, Freitas, Paulo P., and Cardoso, Susana, Linearization strategies for high sensitivity magnetoresistive sensors, *Eur. Phys. J. Appl. Phys.* **72**, 10601 (2015).
- [27] M. J. Garcia, J. Moulin, S. Wittrock, S. Tsunegi, K. Yakushiji, A. Fukushima, H. Kubota, S. Yuasa, U. Ebels, M. Pannetier-Lecoœur, C. Fermon, R. Lebrun, P. Bortolotti, A. Solignac, and V. Cros, Spin-torque dynamics for noise reduction in vortex-based sensors, *Applied Physics Letters* **118**, 10.1063/5.0040874 (2021).
- [28] F. Matos, R. Macedo, P. P. Freitas, and S. Cardoso, Cofebx layers for mgo-based magnetic tunnel junction sensors with improved magnetoresistance and noise performance, *AIP Advances* **13**, 10.1063/9.0000559 (2023).
- [29] J. Inoue and S. Maekawa, Theory of tunneling magnetoresistance in granular magnetic films, *Physical Review B* **53**, R11927 (1996).
- [30] A. Kawabata, Brownian Motion of a Classical Spin, *Progress of Theoretical Physics* **48**, 2237 (1972).
- [31] K. Miyazaki and K. Seki, Brownian motion of spins revisited, *The Journal of Chemical Physics* **108**, 7052 (1998).
- [32] H. Imamura, H. Arai, R. Matsumoto, T. Yamaji, and H. Tsukahara, Precession dynamics of a small magnet with non-Markovian damping: Theoretical proposal for an experiment to determine the correlation time, *Journal of Magnetism and Magnetic Materials* **553**, 169209 (2022).
- [33] W. F. Brown, Thermal fluctuations of a single-domain particle, *Physical Review* **130**, 1677 (1963).
- [34] R. Kubo, The fluctuation-dissipation theorem, *Reports on Progress in Physics* **29**, 306 (1966).
- [35] H. T. Hardner, M. B. Weissman, M. B. Salamon, and S. S. P. Parkin, Fluctuation-dissipation relation for giant magnetoresistive 1/f noise, *Physical Review B* **48**, 16156 (1993).
- [36] N. Smith, Modeling of thermal magnetization fluctuations in thin-film magnetic devices, *Journal of Applied Physics* **90**, 5768 (2001).
- [37] V. L. Safonov and H. N. Bertram, Nonuniform thermal magnetization noise in thin films: Application to GMR heads, *Journal of Applied Physics* **91**, 7279 (2002).
- [38] A. Ozbay, A. Gokce, T. Flanagan, R. A. Stearrett, E. R. Nowak, and C. Nordman, Low frequency magnetoresistive noise in spin-valve structures, *Applied Physics Letters* **94**, 202506 (2009).